ORGANIC LETTERS

2012
Vol. 14, No. 9
2238–2241

Mechanism and Fluorescence Application of Electrochromism in Photochromic Dithienylcyclopentene

Sumin Lee,[†] Youngmin You,*[,†] Kei Ohkubo,[‡] Shunichi Fukuzumi,*[,†,‡] and Wonwoo Nam*[,†]

Department of Bioinspired Science, Ewha Womans University, Seoul 120-750, Korea, and Department of Material and Life Science, Graduate School of Engineering, Osaka University, ALCA, Japan Science and Technology Agency (JST), Suita, Osaka 565-0871, Japan

odds2@ewha.ac.kr; fukuzumi@chem.eng.osaka-u.ac.jp; wwnam@ewha.ac.kr

Received March 10, 2012

ABSTRACT

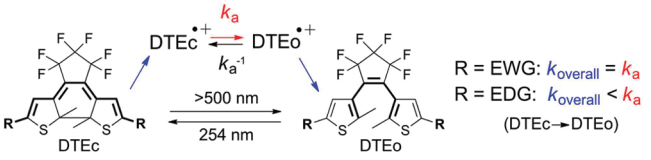

The kinetic process of key intermediates involved in the electrochemical ring opening of photochromic dithienylcyclopentenes (DTEs) has been observed for the first time, where the electronic nature of the DTEs is an important factor that determines the rate-determining step in the electrochromism. The dual chromic property has been implemented to a single molecular fluorescence memory.

Dithienylcyclopentene (DTE) undergoes reversible interconversion under photoirradiation between open and closed form isomers with distinct optical changes. The photochromic DTE derivatives gather enormous research interests because they exhibit ideal properties for molecular switches, such as bistability, thermal irreversibility, and ultrafast conversion.[1−4] Recently, it has been found that some of DTE molecules feature similar conversion in their oxidized or reduced states.[5−7] Such electrochromism of photochromic DTEs is valuable, offering an additional means to address switching states (i.e., open and closed states).[8−14] In fact, the unique dual chromism has been exploited to control memory functions[15−18] and photopolymerization.[19]

In DTE molecules, electrochromism has resemblance to photochromism in that it provides a pathway to bypass a huge ground-state thermodynamic barrier required for isomerization.[20] Previous studies performed by several groups revealed that substituents of the thiophenes have profound consequence to direction of electrochromism

[†] Ewha Womans University.
[‡] Osaka University.

(1) Irie, M. *Chem. Rev.* **2000**, *100*, 1685–1716.
(2) Feringa, B. L. *Molecular Switches*; Wiley-VCH: Weinheim, 2001.
(3) Tian, H.; Yang, S. *Chem. Soc. Rev.* **2004**, *33*, 85–97.
(4) Corredor, C. C.; Huang, Z.-L.; Belfield, K. D. *Adv. Mater.* **2006**, *18*, 2910–2914.
(5) Motoyama, K.; Koike, T.; Akita, M. *Chem. Commun.* **2008**, 5812–5814.
(6) He, B.; Wenger, O. S. *J. Am. Chem. Soc.* **2011**, *133*, 17027–17036.
(7) Léaustic, A.; Anxolabéhère-Mallart, E.; Maurel, F.; Midelton, S.; Guillot, R.; Métivier, R.; Nakatani, K.; Yu, P. *Chem.—Eur. J.* **2011**, *17*, 2246–2255.
(8) Miki, S.; Noda, R.; Fukunishi, K. *Chem. Commun.* **1997**, 925–926.
(9) Kawai, S. H.; Gilat, S. L.; Ponsinet, R.; Lehn, J.-M. *Chem.—Eur. J.* **1995**, *1*, 285–293.
(10) Saika, T.; Iyoda, T.; Honda, K.; Shimidzu, T. *J. Chem .Soc., Perkin Trans. 2* **1993**, 1181–1186.
(11) Newell, A. K.; Utley, J. H. P. *J. Chem. Soc., Chem. Commun.* **1992**, 800–801.
(12) Zhi, J. F.; Baba, R.; Hashimoto, K.; Fujishima, A. *J. Photochem. Photobiol., A* **1995**, *92*, 91–97.
(13) Ikeda, H.; Sakai, A.; Namai, H.; Kawabe, A.; Mizuno, K. *Tetrahedron Lett.* **2007**, *48*, 8338–8342.
(14) Iyoda, T.; Saika, T.; Honda, K.; Shimidzu, T. *Tetrahedron Lett.* **1989**, *30*, 5429–5432.
(15) Areephong, J.; Browne, W. R.; Katsonis, N.; Feringa, B. L. *Chem. Commun.* **2006**, 3930–3932.
(16) Baron, R.; Onopriyenko, A.; Katz, E.; Lioubashevski, O.; Willner, I.; Wang, S.; Tian, H. *Chem. Commun.* **2006**, 2147–2149.
(17) Xie, N.; Chen, Y. *New J. Chem.* **2006**, *30*, 1595–1598.
(18) Lin, H.; Wei, Z.; Xiang, J.; Xu, W.; Zhu, D. *ChemPhysChem* **2009**, *10*, 1996–1999.

10.1021/ol300604n
Published on Web 04/26/2012

(i.e., ring opening vs ring closing).[21,22] In contrast to well-established photochromism,[1,23] however, key intermediates in the electrochromic processes have yet to be fully elucidated to date. For example, the Branda,[24–27] Launay,[28] and Irie[22] groups identified radical cations as being responsible for oxidative ring opening or closing reactions, whereas the Feringa group proposed that the reactions proceed via dicationic states.[29] Furthermore, the rate-determining step in the electrochromism involving electron transfer, isomerization, and back electron transfer has not been established. Since the dual chromic properties hold great promise for key applications in multifunctional molecular devices, knowledge of mechanistic details is of central importance.

In this study, the kinetics of oxidative ring-opening reactions (i.e., $c \rightarrow c^{\bullet+} \rightarrow o^{\bullet+} \rightarrow o$; c and o stand for closed and open forms, respectively) of a series of DTE compounds has been investigated by performing stopped-flow UV−vis absorption measurements. The direct spectroscopic studies establish that rates for isomerization of the key intermediates (i.e., $c^{\bullet+} \rightarrow o^{\bullet+}$) are increased by electron-rich groups, whereas overall reaction rates display an opposite trend. The unique dual chromic functionality has been further implemented to a single molecular switch, demonstrating bistable fluorescence memory.

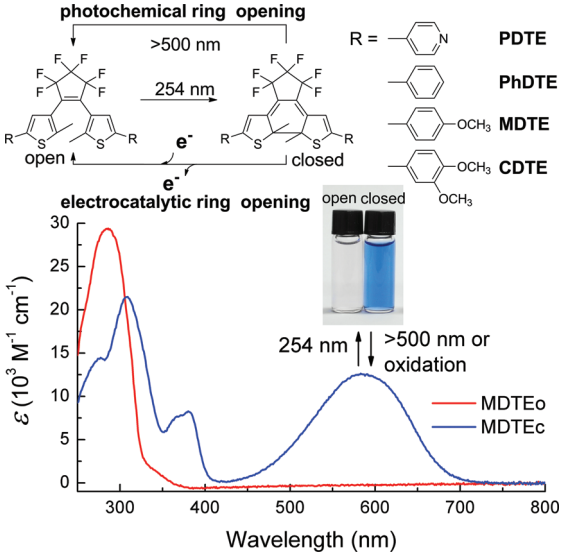

Figure 1. Structures of the open and closed forms of DTE compounds and UV−vis absorption spectra displaying the photo- and electrochromism of MDTE. Inset photo: CH_3CN solutions of open (left) and closed (right) forms of 10 μM MDTE.

Figure 1 displays dual chromism of DTEs. In order to investigate electronic influence in the electrochromic processes, four DTE compounds were prepared by introducing pyridyl (PDTE),[30,31] phenyl (PhDTE),[32] 4-methoxyphenyl (MDTE),[29] and 3,4-dimethoxyphenyl (CDTE) at the 2-position of thiophene rings. The compounds were fully characterized with standard identification methods, and the results fully agreed with the proposed structures (Supporting Information, Materials and Experimental Details). The DTE molecules undergo efficient photochromic interconversion between a closed form (DTEc) and an open form (DTEo) under alternating photoirradiation at 254 and >500 nm, respectively. Photophysical data including photochromic conversion yields and photochromic quantum yields are listed in Supporting Information, Table S1.

Addition of oxidants, such as $Cu(ClO_4)_2$ (E_p(ox) = 1.09 V vs SCE), $[Fe(bpy)_3](PF_6)_3$ ($E_{1/2}$(redox) = 1.06 V vs SCE), and $[Ru(bpy)_3](ClO_4)_3$ ($E_{1/2}$(redox) = 1.26 V vs SCE), to acetonitrile (CH_3CN) solutions containing 50 μM closed form of DTE compounds bleached the characteristic blue absorption color of the closed form (Figure 1 and Supporting Information, Figure S1),[27] indicating occurrence of ring-opening reactions (see Supporting Information, Figure S2 for ^{1}H NMR spectra). The ring opening is due to oxidation of DTEc because electron transfer from DTEc to the oxidants is thermodynamically favored as judged by the oxidation potentials of DTEc (Table 1). The oxidation of DTEs generated radical cations ($DTEc^{\bullet+}$) as supported by distinct ESR signals of CH_3CN solutions of PhDTE, MDTE, and CDTE in the presence of 1 equiv of $[Ru(bpy)_3](PF_6)_3$ (Supporting Information, Figure S3). A second oxidation to a dication of the closed form ($DTEc^{2+}$) was not observed in the cyclic voltammograms until the end of the oxidation of the open form (Supporting Information, Figure S4). The oxidative ring opening is efficient with conversion yields larger than 88%, as determined by ^{1}H NMR spectroscopy (Table 1).

Table 1. Electrochemical and Kinetic Data of DTE Compounds

	E_p(ox) (V, vs SCE)[a]					
	open	closed	k_{obs} (s^{-1})[b] $c^{\bullet+}\rightarrow o^{\bullet+}$	k_{obs} (s^{-1})[b] overall	spin density[c]	opening yield (%)[d]
PDTE	ND[e]	1.05	0.058	0.058	0.0596	quant
PhDTE	1.54	0.90	0.071	0.037	0.0529	90
MDTE	1.24	0.72	0.33	0.0063	0.0465	88
CDTE	1.15	0.69	2.1	0.00014	0.0463	quant

[a] Pt disk working electrode and Pt wire counter electrode; $Ag/AgNO_3$ pseudo reference electrode; 0.1 M n-Bu_4NPF_6 and 1 mM DTE compound in deaerated CH_3CN; scan rate = 100 mV/s. [b] 50 μM DTE + 4 equiv $Cu(ClO_4)_2$ at 10 °C. [c] Quantum chemically calculated spin-density of the cleaved C−C bond. See Supporting Information for details. [d] Determined by ^{1}H NMR. [e] Not detected.

(19) Areephong, J.; Kudernac, T.; de Jong, J. J. D.; Carroll, G. T.; Pantorott, D.; Hjelm, J.; Browne, W. R.; Feringa, B. L. *J. Am. Chem. Soc.* **2008**, *130*, 12850–12851.

(20) Staykov, A.; Areephong, J.; Browne, W. R.; Feringa, B. L.; Yoshizawa, K. *ACS Nano* **2011**, *5*, 1165–1178.

(21) Browne, W. R.; de Jong, J. J. D.; Kudernac, T.; Walko, M.; Lucas, L. N.; Uchida, K.; van Esch, J. H.; Feringa, B. L. *Chem.—Eur. J.* **2005**, *11*, 6430–6441.

(22) Moriyama, Y.; Matsuda, K.; Tanifuji, N.; Irie, S.; Irie, M. *Org. Lett.* **2005**, *7*, 3315–3318.

(23) Nakamura, S.; Yokojima, S.; Uchida, K.; Tsujioka, T.; Goldberg, A.; Murakami, A.; Shinoda, K.; Mikami, M.; Kobayashi, T.; Kobatake, S.; Matsuda, K.; Irie, M. *J. Photochem. Photobiol., A* **2008**, *200*, 10–18.

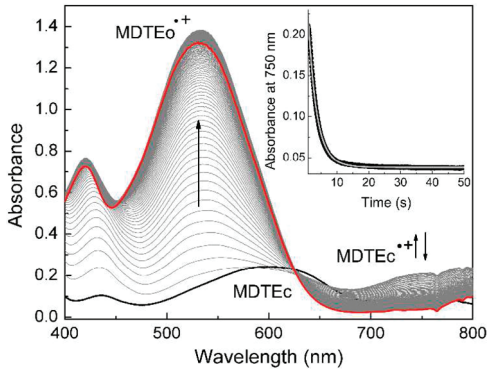

Figure 2. Stopped-flow UV−vis absorption spectra of 50 μM MDTEc (CH_3CN) after the addition of 200 μM $Cu(ClO_4)_2$ (CH_3CN) at 10 °C: black, before the addition of $Cu(ClO_4)_2$; red, 50 s after the addition of $Cu(ClO_4)_2$. Inset graph is a decay trace of $MDTEc^{\bullet+}$ observed at 750 nm.

Reactions of $DTEc^{\bullet+}$ were monitored by stopped-flow UV−vis absorption spectroscopy employing a single-mixing technique. As shown in Figure 2, a broad absorption band around 750 nm appears immediately after the addition of 200 μM $Cu(ClO_4)_2$ to 50 μM MDTEc (CH_3CN, 10 °C). The absorption band is bathochromically shifted relative to the neutral form (MDTEc, 593 nm), which is consistent with a predicted UV−vis absorption spectrum for $MDTEc^{\bullet+}$ (TD-DFT, uB3LYP/6-311+G(d,p); Supporting Information, Figure S5). The 750 nm band of $MDTEc^{\bullet+}$ obeys a monoexponential decay with a concomitant rise of new absorption bands at 534 and 420 nm, which originate from a radical cation of an open form ($MDTEo^{\bullet+}$). TD-DFT calculations also support $MDTEo^{\bullet+}$ being responsible for these absorption bands. In addition, nearly identical UV−vis absorption changes were observed when the oxidative reaction was triggered by $[Fe(bpy)_3](PF_6)_3$ or electrolysis at 0.89 V (Supporting Information, Figures S6 and S7). The presence of a clear isosbestic point at 627 nm indicates the conversion of $MDTEc^{\bullet+} \rightarrow MDTEo^{\bullet+}$ without further oxidations or byproduct formation. PDTE, PhDTE, and CDTE display similar spectral behaviors (Supporting Information, Figure S8), indicating the identical cycloreversion in the cyclohexatriene core (i.e., $DTEc^{\bullet+} \rightarrow DTEo^{\bullet+}$).

(24) Gorodetsky, B.; Branda, N. R. *Adv. Funct. Mater.* **2007**, *17*, 786–796.
(25) Gorodetsky, B.; Samachetty, H. D.; Donkers, R. L.; Workentin, M. S.; Branda, N. R. *Angew. Chem., Int. Ed.* **2004**, *43*, 2812–2815.
(26) Peters, A.; Branda, N. R. *Chem. Commun.* **2003**, 954–955.
(27) Peters, A.; Branda, N. R. *J. Am. Chem. Soc.* **2003**, *125*, 3404–3405.
(28) Guirado, G.; Coudret, C.; Hliwa, M.; Launay, J.-P. *J. Phys. Chem. B* **2005**, *109*, 17445–17459.
(29) Browne, W. R.; de Jong, J. J. D.; Kudernac, T.; Walko, M.; Lucas, L. N.; Uchida, K.; van Esch, J. H.; Feringa, B. L. *Chem.—Eur. J.* **2005**, *11*, 6414–6429.
(30) Gilat, S. L.; Kawai, S. H.; Lehn, J. M. *J. Chem. Soc., Chem. Commun.* **1993**, 1439–1442.
(31) Samachetty, H. D.; Branda, N. R. *Chem. Commun.* **2005**, 2840–2842.
(32) Irie, M.; Lifka, T.; Kobatake, S.; Kato, N. *J. Am. Chem. Soc.* **2000**, *122*, 4871–4876.

As summarized in Table 1, reaction rates for $DTEc^{\bullet+} \rightarrow DTEo^{\bullet+}$ heavily depend on the nature of the attached aryl rings. Electron-rich CDTE showed the fastest conversion, whereas electron-deficient PDTE featured a slow ring opening. This tendency can be understood in the light of the calculated spin density of the cleaved C−C bond between two thiophene rings (Table 1). Since SOMO (singly occupied molecular orbital) of $DTEc^{\bullet+}$ contains a bonding orbital interaction of the C−C bond (Supporting Information, Figure S9),[20] a smaller spin density value implies an increased probability for ring opening. The effect becomes more pronounced by delocalization of the unpaired electron by substituents such as the 3,4-dimethoxyphenyl group, resulting in the faster ring opening of CDTE. In contrast, the overall reaction (i.e., DTEc → $DTEc^{\bullet+} \rightarrow DTEo^{\bullet+} \rightarrow$ DTEo) of CDTE is the slowest among the tested DTE compounds. The overall reaction rate constant of CDTE was 1.4×10^{-4} s^{-1}, whereas PDTE exhibited the fastest ring opening with a reaction rate constant of 5.8×10^{-2} s^{-1} (Table 1 and Supporting Information, Figure S10). We consider that an equilibration back to $DTEc^{\bullet+}$ (i.e., $DTEo^{\bullet+} \rightarrow DTEc^{\bullet+}$) becomes dominant or a reductive back electron transfer (i.e., $DTEo^{\bullet+} \rightarrow$ DTEo) is retarded in the case of electron-rich DTEs.[33] In fact, slower back electron transfer to $CDTEo^{\bullet+}$ is predicted from the lowest oxidation potential (Table 1). Therefore, there is a kinetic trade-off between the isomerization and the rest of reaction processes including back electron transfer or an equilibrium between radical intermediates. Based on the calculation, spectroscopic, and electrochemical results, a reaction mechanism is proposed in Scheme 1.

Scheme 1. Mechanism of the Electrocatalytic Ring Opening of DTE Compounds

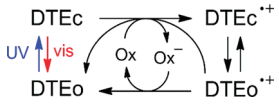

With the understanding of the electrochromism of photochromic DTEs, utility of the dual chromism has been extended to fluorescence memory (SM1). For this purpose, red-fluorescent rhodamines were introduced to MDTE via ester linkages (Figure 3, refer to Supporting Information for synthetic details). In the closed state of SM1 (SM1c), photoexcitation of rhodamine (λ_{ex} = 495 nm) produced weak fluorescence emission due to nonradiative fluorescence-resonance energy transfer (FRET) to the MDTEc moiety. The UV−vis absorption spectrum of SM1c is summation of the absorption spectra of MDTEc and rhodamine, revealing the absence of any ground-state electronic interaction (Figure 3). Oxidative ring opening by

(33) The electron-rich CDTE and MDTE display temperature dependence in their overall reaction rate constants stronger than that of PDTE, which suggests equilibrium favored to the radical cation of closed forms in the case of electron-rich DTEs. Refer to Supporting Information, Figure S16.

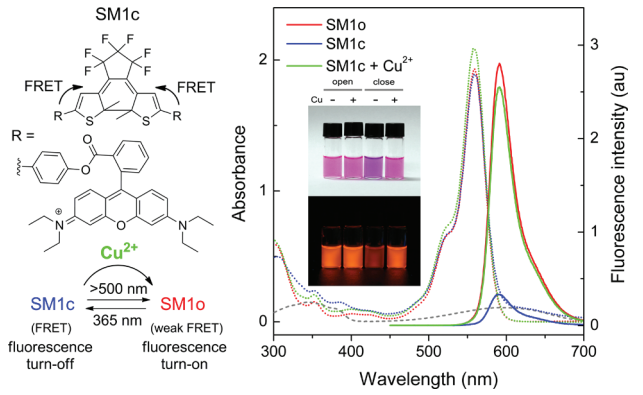

Figure 3. Fluorescence turn-on by the oxidative ring opening of SM1. UV−vis absorption (dotted line) and fluorescence (solid line) spectra of an open form (red), a closed form (blue), and a closed form in the presence of 3 equiv of $Cu(ClO_4)_2$ (green) of 10 μM SM1 (CH_3CN) are shown. The UV−vis absorption spectrum of a closed form of MDTE is included for comparison (gray).

Table 2. Spectroscopic Data of SM1[a]

	λ_{ems} (nm) (PLQY, %)[b]	τ_{fl} (ns)[c]	PCQY (%)[d]	conversion yield (%)[e] photo	conversion yield (%)[e] electro[f]
open	591 (22)	1.57	33 (o → c)	60 (o → c)	NR[g] (o → c)
closed	590 (3.3)	1.39	2.0 (c → o)	48 (c → o)	85 (c → o)

[a] 10 μM in CH_3CN. [b] Photoluminescence quantum yield (λ_{ex} = 495 nm). [c] Fluorescence lifetime (λ_{ex} = 450 nm; λ_{obs} = 590 nm). [d] Photochromic quantum yield. [e] Determined by ^1H NMR. [f] Oxidant = $Cu(ClO_4)_2$ (1 equiv). [g] No reaction.

$Cu(ClO_4)_2$ or photoirradiation at > 500 nm eliminated the characteristic absorption band of MDTEc, while the absorption band of rhodamine was intact. Conversion yields for the photochromic and electrochromic ring opening are 48% and 85%, respectively (Table 2). The opening of SM1 turns on the fluorescence intensity with an on/off ratio of 7 due to decreased spectral overlap between the absorption and the fluorescence emission bands. Suppression of the nonradiative FRET in the open state of SM1 (SM1o) is supported by an increase in the photoluminescence lifetime from 1.39 μs (SM1c) to 1.57 μs (SM1o). The fluorescence modulation is reversible because photoirradiation at 365 nm regenerated SM1c with a conversion yield of 60% in the presence of a metal chelator such as *N*,*N*,*N*′,*N*′-tetrakis(2-picolyl)ethylenediamine (TPEN).[34] The fluorescence on/off memory function of SM1 can be therefore accomplished by a combination of photochromism and electrochromism. Specifically, a write process by oxidation sets the "fluorescence-on" state. Read-out of the fluorescence information can be done by photoexcitation at 495 nm, which does not evoke photochromic ring opening of SM1 (Supporting Information, Figure S15). Finally, ring closing by photoirradiation at 365 nm is employed for an erasure process to set the "fluorescence-off" state, completing a full memory process, and this can be repeated many times (Figure 4). The unique advantage of this system is the additional addressability, which enables nondestructive read-out because undesirable crosstalks between the read-out and the write processes are inherently prohibited.

(34) Coordination of Cu(II) to TPEN induces a large negative shift of the one-electron reduction potential when no cathodic peak was observed within 0.4−1.2 V (vs SCE). In such a case, Cu(II) does not act as a one-electron oxidant for DTEc.

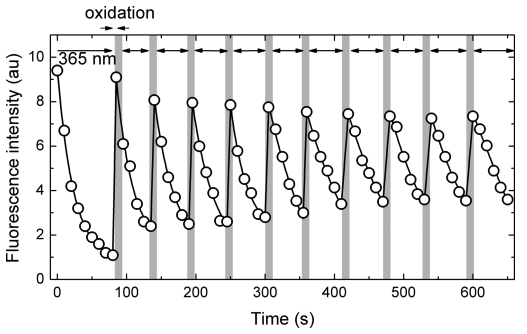

Figure 4. Fluorescence switching of 10 μM SM1 (CH_3CN) by alternating photochromism (λ_{irr} = 365 nm + 1 equiv of TPEN) and electrochromism (oxidant = 1 equiv of $Cu(ClO_4)_2$).

In summary, the electrochemical ring opening step in photochromic DTE compounds has been spectroscopically observed. The kinetic studies revealed that the electronic nature of the DTEs is the key factor that governs the rate-determining step in the overall ring-opening reaction. The dual chromic property was implemented to demonstrate bistable fluorescence memory functions. Modulation of intramolecular FRET between the DTE moiety and fluorescent rhodamine was successfully accomplished by the combination of electrochromism and photochromism.

Acknowledgment. This work was supported by CRI, GRL (2010-00353), and WCU program (R31-2008-000-10010-0) (W.N.) from the NRF, Korea, Grants-in-Aid (nos. 20108010 and 23750014) (S.F. and K.O.) a Global COE program from the JSPS, Japan, and RP-Grant 2010 (Y.Y.) of Ewha Womans University.

Supporting Information Available. Synthesis and experimental details; Figures S1−S39; Tables S1and S2. This material is available free of charge via the Internet at http://pubs.acs.org.

The authors declare no competing financial interest.